

Infrared Spectroscopic and Density Functional Theory Studies on the Reactions of Zinc and Cadmium Atoms with Ammonia

Ling Jiang and Qiang Xu*

National Institute of Advanced Industrial Science and Technology (AIST), Ikeda, Osaka 563-8577

Graduate School of Science and Technology, Kobe University, Nada-ku, Kobe 657-8501

Received April 12, 2006; E-mail: q.xu@aist.go.jp

Reactions of zinc and cadmium atoms with ammonia molecules in a solid argon matrix have been studied by infrared spectroscopy. MNH_3 (M = Zn and Cd) was found from the reaction of ammonia with excited metal atoms, similar to the reaction of ammonia with Hg atom, but quite different from those with other metal atoms (Sc, Ti, V, etc.). The absorptions peaks of $HZnNH_2$ sharply increased upon broad-band irradiation, whereas there was no detectable $HCdNH_2$ produced under the same experimental conditions. Density functional theory calculations were performed on these molecules and the transition states. The agreement between experimental and calculated vibrational frequencies, relative absorption intensities, and isotopic shifts provides strong support for the identification of the products. Furthermore, energetic analysis for possible reaction paths of these reactions is also given.

The interaction of ammonia with transition-metal atoms and main group elements is of considerable interest due to its importance in many catalytic processes such as carbonylation or alkylation of ammonia and amines.[1] Recently, it has been found that for the early transition-metal atoms (Sc, Ti, and V), the MNH_3 complexes, generated from the reactions of ground-state metal atoms with NH_3, undergo photochemical rearrangement to the inserted $HMNH_2$ complexes and then to ScNH and H_2MNH (M = Ti and V) after ultraviolet–visible irradiation.[2] For the middle and late transition-metal atoms (Fe, Ni, and Cu), metal atoms react with NH_3 molecules to form the MNH_3 complexes, and ultraviolet–visible irradiation induces the insertion of the metals into a N–H bond with affording the amido derivatives $HMNH_2$ (M = Fe, Ni, and Cu), $HMNH_2NH_3$ (M = Fe or Ni), and H + MNH_2 (M = Cu).[3–5] In the case of the reactions of NH_3 with main group metal atoms, $HMNH_2$ prefers to lose one H atom to form monovalent MNH_2 complexes; however, H_2 elimination occurs when M = Si and Ge.[6] The difference in photochemical behavior of $HMNH_2$ complexes is a direct consequence of the valence-electron configurations of the M atoms.[2] On the other hand, laser-induced fluorescence and action spectroscopy coupled with isotopic studies shows that a Hg–NH_3 excimer is formed from the reaction of NH_3 molecules with an excited Hg ($^3P_1$) atom.[7] Two triplet states, ^3E and $^3A_1$, have been found experimentally for Hg–NH_3.[7] Theoretically, the oxidative addition of ammonia to second row transition-metal atoms have been studied, and the lowest barriers for N–H insertion were found for the atoms to the left with values slightly below zero.[8]

Recent studies have shown that, with the aid of isotopic substitution techniques, matrix isolation infrared spectroscopy combined with quantum chemical calculation is very powerful for investigating structure and bonding of novel species.[2–6,9,10] Here, we report our results for the reactions of NH_3 molecules with zinc and cadmium atoms in a solid-argon matrix. IR spectroscopy and theoretical calculations provide evidence for the formation of MNH_3 (M = Zn and Cd) and the insertion of zinc atom into a N–H bond.

Experimental and Theoretical Procedures

The experimental procedures for laser ablation and matrix isolation infrared spectroscopy were similar to those previously reported.[11] Briefly, the Nd:YAG laser fundamental (1064 nm, 10 Hz repetition rate with 10 ns pulse width) was focused on rotating Zn and Cd targets. The laser-ablated metal atoms then co-deposited with NH_3 in excess argon onto a CsI window cooled usually to 7 K by means of a closed-cycle helium refrigerator. Typically, 1–5 mJ/pulse laser power was used. NH_3 (19.5%, balanced with Ar), $^{15}NH_3$ (99%) and ND_3 (99%) were used to prepare the NH_3/Ar mixtures. In general, matrix samples were deposited for one to two hours with a typical deposition rate of 2–4 mmol per hour. After sample deposition, IR spectra were recorded on a BIO-RAD FTS-6000e spectrometer at 0.5 cm^{-1} resolution using a liquid nitrogen cooled HgCdTe (MCT) detector for the spectral range of 5000–400 cm^{-1}. Samples were annealed at different temperatures and subjected to broad-band irradiation ($\lambda > 250$ nm) using a high-pressure mercury arc lamp (Ushio, 100 W).

Quantum chemical calculations were performed to predict the structures and vibrational frequencies of the observed reaction products using Gaussian 03.[12] The B3LYP and MP2 density functional methods were used,[13] and the 6-311+G(d) basis sets were used for C, H, and Zn atoms,[14] and the Los Alamos ECP plus DZ (LANL2DZ) for Cd atoms.[15] Geometries were fully optimized, and vibrational frequencies were calculated using analytical second derivatives. Transition-state optimizations were done using the QST3 algorithm as part of the synchronous transit-guided quasi-Newton (STQN) method, followed by vibrational calculations to show that the obtained structures were true saddle points. The intrinsic reaction coor-

Published on the web October 10, 2006; doi:10.1246/bcsj.79.1519

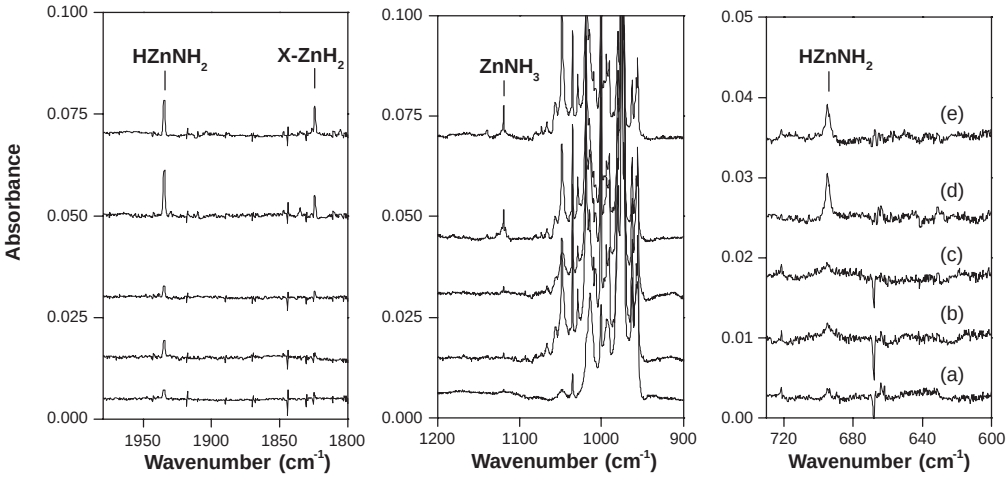

Fig. 1. Infrared spectra in the 2000–1800, 1200–900, and 720–600 cm^{-1} regions from the co-deposition of laser-ablated Zn atoms with 0.5% NH_3 in Ar. (a) 1 h of sample deposition at 7 K, (b) after annealing to 25 K, (c) after annealing to 30 K, (d) after 15 min of broad-band irradiation, and (e) after annealing to 34 K. The absorptions around 1000 cm^{-1} are due to the NH_3 molecules.

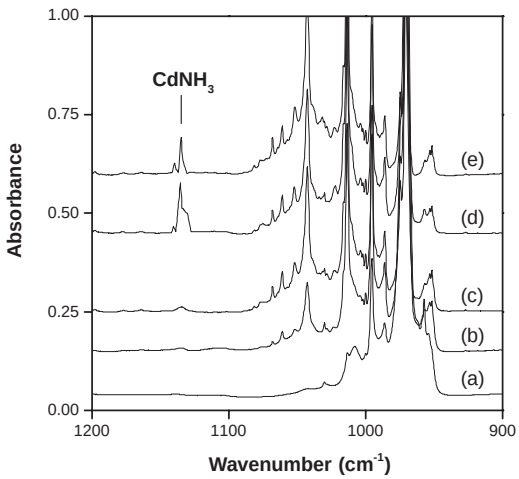

Fig. 2. Infrared spectra in the 1200–900 cm^{-1} region from the co-deposition of laser-ablated Cd atoms with 0.5% NH_3 in Ar. (a) 1 h of sample deposition at 7 K, (b) after annealing to 25 K, (c) after annealing to 30 K, (d) after 15 min of broad-band irradiation, and (e) after annealing to 34 K.

dinate (IRC) method was used to track minimum energy paths from transition structures to the corresponding local minima. A step size of 0.1 $amu^{1/2}$ bohr was used for the IRC procedure. Previous investigations have shown that this computational scheme can provide reliable information for the reactions of ammonia with metal atoms, such as infrared frequencies, relative absorption intensities, and isotopic shifts.[2–6]

Results and Discussion

Experiments have been done with NH_3 molecules at concentrations ranging from 0.02 to 1.0% in excess argon. Selected regions of typical infrared spectra for the reactions of laser-ablated Zn and Cd atoms with NH_3 molecules in excess argon are shown in Figs. 1 and 2, respectively, and the absorption bands in different isotopic experiments are listed in Table 1. Stepwise annealing and photolysis behavior of the product absorptions are also shown in the figures and will be discussed below.

Table 1. Infrared Absorptions (cm^{-1}) from the Co-Deposition of Laser-Ablated Zn and Cd Atoms with Ammonia in Excess Argon at 7 K

$^{14}NH_3$	$^{15}NH_3$	ND_3	Assignment
1934.9	1934.9	1389.1	$HZnNH_2$, ν(Zn–H)
1824.4	1824.4		$X–ZnH_2$, ν(Zn–H)
1118.8	1113.4	858.9	$ZnNH_3$, $\delta_{sym}(NH_3)$
694.9	681.2	656.5	$HZnNH_2$, ν(Zn–NH_2)
1139.3	1135.6	889.5	$CdNH_3$, $\delta_{sym}(NH_3)$

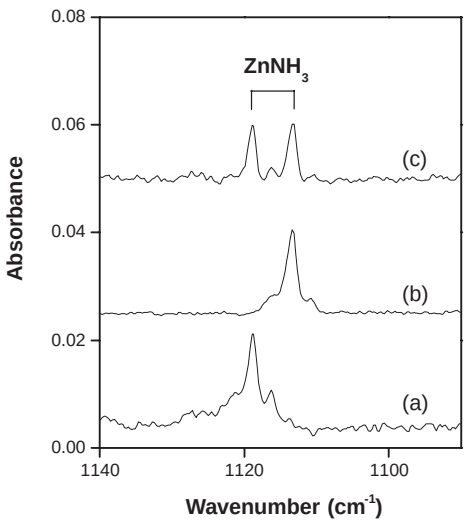

Fig. 3. Infrared spectra in the 1140–1080 cm^{-1} region from the co-deposition of laser-ablated Zn atoms with isotopic NH_3 in Ar after annealing to 34 K. (a) 0.5% $^{14}NH_3$, (b) 0.5% $^{15}NH_3$, and (c) 0.25% $^{14}NH_3$ + 0.25% $^{15}NH_3$.

Quantum chemical calculations have been carried out for the possible isomers and electronic states of the potential products. Figure 4 shows the optimized structures of the isomers and transition states of MNH_3. Tables 2 and 3 list the vibra-

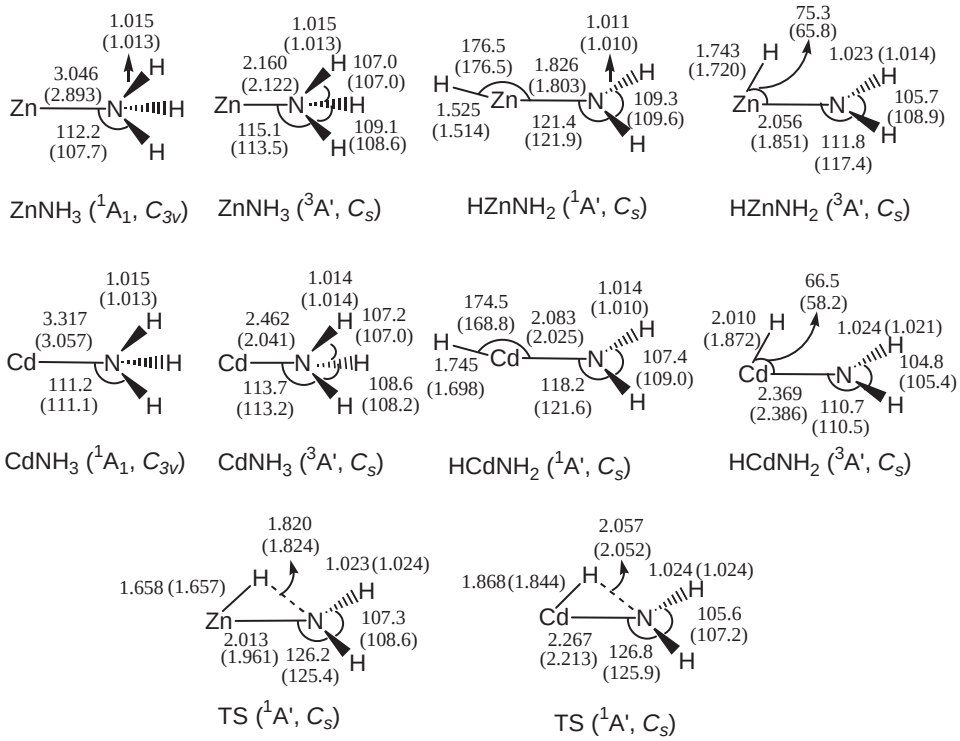

Fig. 4. Optimized structures with bond lengths (Å) and bond angles (°) of the MNH_3 (M = Zn and Cd) isomers and the transition states calculated at the B3LYP and MP2 (in parentheses) levels.

Table 2. Vibrational Frequencies (cm^{-1}) and Intensities ($km\,mol^{-1}$) for the Reaction Intermediates, Products, and Transition States from the Reactions of Zn and Cd Atoms with NH_3 Calculated at the B3LYP Level

Species	Frequency (intensity)
$ZnNH_3$ ($^1A_1$)	3592.4 (3 × 2, e), 3465.1 (6, a_1), 1729.6 (34 × 2, e), 1091.9 (208, a_1), 163.4 (27 × 2, e), 62.5 (5, a_1)
$ZnNH_3$ ($^3A'$)	3563.9 (827, a′), 3532.6 (116, a″), 3460.4 (379, a′), 1705.3 (50, a′), 1602.3 (159, a″), 1214.0 (126, a′), 499.4 (19, a″), 449.8 (301, a′), 311.3 (11, a′)
$HZnNH_2$ ($^1A'$)	3639.0 (10, a″), 3549.6 (2, a′), 1950.7 (116, a′), 1613. 3 (19, a′), 733.1 (71, a″), 660.9 (43, a′), 492.9 (30, a′), 462.7 (44, a″), 268.0 (207, a′)
$HZnNH_2$ ($^3A'$)	3512.8 (4, a″), 3415.8 (2, a′), 1607.4 (35, a′), 1153.1 (207, a′), 727.0 (179, a′), 646.7 (0.4, a″), 496.2 (163, a′), 318.7 (1, a′), 260.8 (20, a″)
TS ($^1A'$)	3520.5 (1, a″), 3404.7 (14, a′), 1572.0 (22, a′), 1462.4 (15, a′), 716.5 (54, a″), 687.9 (226, a′), 432.1 (82, a′), 283.2 (0.3, a″), 1077.6*i* (819, a′)
$CdNH_3$ ($^1A_1$)	3593.6 (3 × 2, e), 3465.9 (8, a_1), 1733.2 (36 × 2, e), 1092.0 (242, a_1), 140.9 (27 × 2, e), 52.1 (3, a_1)
$CdNH_3$ ($^3A'$)	3596.2 (105, a′), 3555.5 (0.4, a″), 3481.3 (6, a′), 1717.7 (30, a′), 1521.5 (1, a″), 1183.5 (176, a′), 442.0 (4, a″), 381.3 (32, a′), 263.1 (5, a′)
$HCdNH_2$ ($^1A'$)	3594.7 (2, a″), 3504.8 (2, a′), 1674.8 (227, a′), 1608.6 (7, a′), 700.4 (67, a″), 539.6 (49, a′), 402.7 (64, a′), 377.3 (184, a′), 356.4 (80, a″)
$HCdNH_2$ ($^3A'$)	3496.3 (1, a″), 3401.5 (1, a′), 1603.4 (31, a′), 965.6 (230, a′), 681.9 (178, a′), 567.9 (2, a″), 434.5 (173, a′), 251.7 (0.8, a′), 248.8 (39, a″)
TS ($^1A'$)	3496.9 (0.3, a″), 3393.7 (23, a′), 1589.0 (21, a′), 1340.3 (27, a′), 683.6 (233, a′), 610.6 (58, a″), 379.7 (48, a′), 195.6 (0.1, a″), 857.8*i* (582, a′)

tional frequencies and intensities calculated at the B3LYP and MP2 levels, respectively, and Table 4 is a comparison of the observed and calculated isotopic frequency ratios of the reaction products. Figure 5 illustrates potential energy surfaces for the Zn + NH_3 and Cd + NH_3 reactions.

MNH_3 Molecule. A weak absorption at 1118.8 cm^{-1} in the Zn + NH_3 experiments appeared after sample deposition, slightly increased on sample annealing, markedly increased after broad-band irradiation, and slightly increased after further higher temperature annealing (Fig. 1). The 1118.8 cm^{-1} band

Table 3. Vibrational Frequencies (cm^{-1}) and Intensities ($km\,mol^{-1}$) for the Reaction Intermediates, Products, and Transition States from the Reactions of Zn and Cd Atoms with NH_3 Calculated at the MP2 Level

Species	Frequency (intensity)
$ZnNH_3$ ($^1A_1$)	3668.1 (10 × 2, e), 3514.7 (2, a_1), 1740.1 (38 × 2, e), 1142.1 (238, a_1), 182.6 (19 × 2, e), 75.3 (9, a_1)
$ZnNH_3$ ($^3A'$)	3658.1 (209, a′), 3604.3 (2, a″), 3518.4 (17, a′), 1728.7 (11, a′), 1543.8 (0.01, a″), 1278.9 (193, a′), 563.2 (10, a″), 330.8 (14, a′), 184.8 (7, a′)
$HZnNH_2$ ($^1A'$)	3706.2 (21, a″), 3600.7 (8, a′), 2004.5 (110, a′), 1643.7 (23, a′), 750.7 (84, a″), 686.0 (44, a′), 495.0 (32, a′), 461.9 (53, a″), 301.0 (225, a′)
$HZnNH_2$ ($^3A'$)	3663.6 (13, a″), 3549.0 (3, a′), 1624.9 (33, a′), 701.3 (1, a′), 617.1 (39, a′), 431.0 (151, a″), 23.8 (0, a′), 21.1 (23, a′), 5.9 (0.3, a″)
TS ($^1A'$)	3565.2 (9, a″), 3424.8 (13, a′), 1579.2 (15, a′), 1505.4 (15, a′), 726.0 (63, a″), 683.5 (269, a′), 478.7 (56, a′), 274.9 (8, a″), 983.2*i* (567, a′)
$CdNH_3$ ($^1A_1$)	3671.4 (10 × 2, e), 3517.8 (4, a_1), 1746.7 (39 × 2, e), 1148.3 (268, a_1), 183.2 (18 × 2, e), 67.1 (7, a_1)
$CdNH_3$ ($^3A'$)	3668.5 (73, a′), 3624.6 (1, a″), 3526.4 (13, a′), 1731.7 (34, a′), 1476.7 (31, a″), 1256.2 (205, a′), 494.3 (38, a″), 280.8 (14, a′), 206.0 (10, a′)
$HCdNH_2$ ($^1A'$)	3695.6 (14, a″), 3591.7 (3, a′), 1819.1 (151, a′), 1628.0 (12, a′), 702.4 (97, a″), 563.9 (52, a′), 440.6 (32, a′), 409.9 (67, a′), 304.9 (245, a″)
$HCdNH_2$ ($^3A'$)	3584.8 (7, a″), 3472.5 (1, a′), 1631.6 (44, a′), 1266.7 (244, a′), 711.4 (233, a′), 567.8 (2, a″), 407.3 (329, a′), 250.6 (34, a′), 127.7 (35, a″)
TS ($^1A'$)	3554.2 (3, a″), 3422.9 (19, a′), 1588.4 (11, a′), 1404.6 (25, a′), 697.1 (290, a′), 635.4 (66, a″), 416.0 (34, a′), 182.7 (3, a″), 878.7*i* (752, a′)

Table 4. Comparison of the Observed and Calculated (B3LYP Level) Isotopic Frequency Ratios of the Reaction Products

		$^{14}N/^{15}N$		H/D	
Species	Mode	Obsd	Calcd	Obsd	Calcd
$ZnNH_3$	$\delta_{sym}(NH_3)$	1.0049	1.0053	1.3026	1.3155
$CdNH_3$	$\delta_{sym}(NH_3)$	1.0033	1.0038	1.2808	1.3136
$HZnNH_2$	ν(Zn–H)	1.0000	1.0001	1.3929	1.4028
$HZnNH_2$	ν(Zn–NH_2)	1.0201	1.0237	1.0585	1.0610

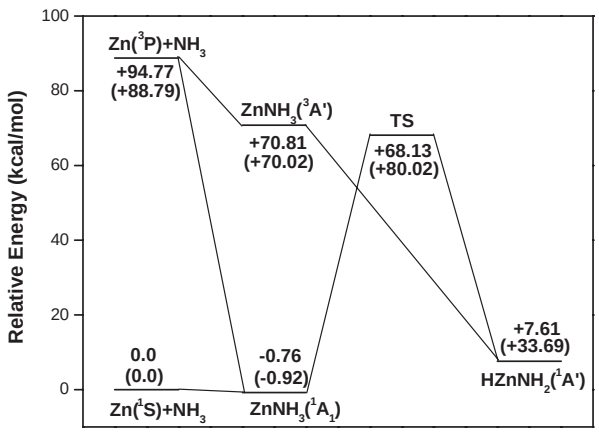

Fig. 5. Potential energy surface following the reaction path from Zn + NH_3 leading to the products (B3LYP level). Energies given are in kcal mol^{-1}, and the corresponding values for Cd are listed in parentheses.

shifted to 1113.4 cm^{-1} with $^{15}NH_3$ and to 858.9 cm^{-1} with ND_3 with an isotopic $^{14}N/^{15}N$ ratio of 1.0049 and H/D ratio of 1.3026, which are close to the corresponding ratios ($^{14}N/^{15}N$: 1.0043 and H/D ratio: 1.2820) of the ν_2 mode of the NH_3 monomer in an argon matrix.[16] In the mixed $^{14}NH_3 + {}^{15}NH_3$ isotopic spectra (Fig. 3) only the sum of pure isotopic bands was observed, which indicates only one NH_3 unit is involved in this mode. Analogous to the previously reported MNH_3 (M = Sc, Ti, V, Fe, Ni, Cu, Al, Si, etc.) complexes,[2–6] the 1118.8 cm^{-1} band was assigned to the symmetric NH_3-bending vibration of the $ZnNH_3$ complex.

Density functional theory (DFT) calculations lend strong support for the assignment. Using the B3LYP results as an example, the $ZnNH_3$ complex was predicted to have C_{3v} symmetry with a $^1A_1$ ground state (Fig. 4) that lies 71.53 kcal mol^{-1} lower in energy than the triplet one. The calculated symmetric NH_3-bending vibration of the $ZnNH_3$ complex was 1091.9 cm^{-1}. At the B3LYP/6-311+G(d) level, the intensity of antisymmetric NH_3-bending vibration (1729.6 cm^{-1}, 34 km mol^{-1}) (Table 2) was much weaker than that of the symmetric one (1091.9 cm^{-1}, 208 km mol^{-1}), in accord with its absence in the present experiments. The calculated $^{14}N/^{15}N$ and H/D ratios of 1.0053 and 1.3155 are consistent with the experimental values, 1.0049 and 1.3026 (Table 4). Good agreement between the experimental and calculated results was also obtained at the MP2 level (Tables 1 and 3). Hereafter, mainly B3LYP results are presented for discussions.

In the Cd + NH_3 experiments, a similar absorption at 1139.3 cm^{-1} was assigned to the symmetric NH_3-bending vibration of the $CdNH_3$ complex, which appeared after broadband irradiation (Fig. 2). This band shifted to 1135.6 cm^{-1} with $^{15}NH_3$ and to 889.5 cm^{-1} with ND_3 with an isotopic $^{14}N/^{15}N$ ratio of 1.0033 and H/D ratio of 1.2808. DFT calculations predict a $^1A_1$ ground state $CdNH_3$ with a symmetric NH_3-bending vibration at 1092.0 cm^{-1}. The calculated $^{14}N/^{15}N$ and H/D ratios of 1.0038 and 1.3136 agree with the experimental values (Table 4).

$HMNH_2$ Molecule. Absorptions at 1934.9 and 694.9 cm^{-1}

in the $Zn + NH_3$ experiments appeared together after sample deposition, slightly increased on sample annealing, and sharply increased after broad-band irradiation (Fig. 1). On the basis of the growth/decay characteristics as a function of changes of experimental conditions, these two bands were determined to be different vibrational modes of the same species. The 1934.9 cm^{-1} band exhibited no nitrogen-15 shift, but shifted to 1389.1 cm^{-1} with ND_3 with a H/D ratio of 1.3929. The band position and isotopic H/D ratio are close to the Zn–H stretching vibration of HZnOH (1955.8 cm^{-1}, H/D ratio: 1.3868 in solid argon),[17] indicating that this band is due to a Zn–H stretching vibration. The 1824.4 cm^{-1} band in Fig. 1 is due to the Zn–H stretching vibration of X–ZnH_2 (X = H_2O, D_2O, N_2, or some other contaminant molecule) as previously reported.[17,18] The 694.9 cm^{-1} band shifted to 681.2 cm^{-1} with $^{15}NH_3$ and 656.5 cm^{-1} with ND_3, giving an isotopic $^{14}N/^{15}N$ ratio of 1.0201 and H/D ratio of 1.0585. This suggests that the band at 694.9 cm^{-1} is due to a Zn–NH_2 stretching mode. Accordingly, the bands at 1934.9 and 694.9 cm^{-1} were assigned to the Zn–H and Zn–NH_2 stretching vibrations of $HZnNH_2$, respectively.

From DFT calculations, $HZnNH_2$ has $^1A'$ ground state with C_s symmetry (Fig. 4). The triplet $HZnNH_2$ molecule was predicted to be 69.20 kcal mol^{-1} in energy higher than the singlet one. The calculated Zn–H and Zn–NH_2 stretching vibrational frequencies of the singlet $HZnNH_2$ molecule (1950.7 and 660.9 cm^{-1}) (Table 2) and isotopic frequency ratios (Table 4) are in accord with the experimental results, supporting the formation of the $HZnNH_2$ species.

In the present experiments on the reaction of laser-ablated Cd atoms with ammonia, however, no absorption for the $HCdNH_2$ products was observed.

Reaction Mechanisms. In the matrix IR spectra, weak IR absorptions due to the MNH_3 (M = Zn and Cd) complexes appeared after sample deposition, slightly increased upon sample annealing, and sharply increased after UV irradiation (Figs. 1 and 2), suggesting that the formation of the MNH_3 complexes is from the reaction of ammonia either with the ground state or with the excited Zn and Cd atoms. However, reaction with the excited atoms should occur to a larger extent. This feature is similar to the reaction of ammonia with the Hg excited atom,[7] but quite different from the reactions with ground state metal atoms such as Sc, Ti, V, etc.[2–6] At the B3LYP/6-311+G(d) level, the formation of the $ZnNH_3$ complex from the reaction of ammonia with the ^1S ground state Zn atom is very slightly exothermic (reaction 1, −0.76 kcal mol^{-1}), but highly exothermic with the ^3P excited Zn atoms (reaction 2, −23.96 kcal mol^{-1} and reaction 3, −71.57 kcal mol^{-1}), in line with the present experiments. Similar results were also obtained for the formation of the $CdNH_3$ complex (reactions 4–6). It was found that ^3P excited metal atoms react with H_2 in the matrix to form group 12 metal hydride molecules.[19] To form the monomethylmetal hydride species, CH_3MH (M = Zn, Cd, and Hg), excitation to the ^3P metal excited state was also required to promote insertion into a methane molecule.[20] Recently, it was reported that the formation of zinc tricarbonyl $Zn(CO)_3$ from the reaction of Zn atoms with CO involves 4s → 4p promotion of the Zn atom.[21] In addition to the aforementioned reports,[7,19–21] the present results show that a number of novel species that have difficulty forming from reactions with ground-state metals are generated using excitation methods such as UV irradiation and laser ablation.

$$Zn\ (^1S) + NH_3 \rightarrow ZnNH_3\ (^1A_1)$$
$$\Delta E = -0.76\ \text{kcal mol}^{-1}\ \text{(B3LYP level)} \quad (1)$$
$$Zn\ (^3P) + NH_3 \rightarrow ZnNH_3\ (^3A')$$
$$\Delta E = -23.96\ \text{kcal mol}^{-1} \quad (2)$$
$$ZnNH_3\ (^3A') \rightarrow ZnNH_3\ (^1A_1)$$
$$\Delta E = -71.57\ \text{kcal mol}^{-1} \quad (3)$$
$$Cd\ (^1S) + NH_3 \rightarrow CdNH_3\ (^1A_1)$$
$$\Delta E = -0.92\ \text{kcal mol}^{-1} \quad (4)$$
$$Cd\ (^3P) + NH_3 \rightarrow CdNH_3\ (^3A')$$
$$\Delta E = -18.77\ \text{kcal mol}^{-1} \quad (5)$$
$$CdNH_3\ (^3A') \rightarrow CdNH_3\ (^1A_1)$$
$$\Delta E = -70.94\ \text{kcal mol}^{-1} \quad (6)$$

Weak IR absorptions for $HZnNH_2$ appeared after sample deposition, slightly increased upon sample annealing, and sharply increased after broad-band photolysis (Fig. 1), implying that there are two possible pathways for the formation of $HZnNH_2$: the rearrangement of singlet $ZnNH_3$ to $HZnNH_2$ (reaction 7) and the direct isomerization of triplet $ZnNH_3$ to $HZnNH_2$ (reaction 9). Both reaction paths require activation energy. As can be seen from Fig. 5, the isomerization of triplet $ZnNH_3$ to singlet $HZnNH_2$ is barrier-free; however, the formation of the triplet $ZnNH_3$ precursor requires activation energy, which supports the above-mentioned analysis. DFT calculations also predicted that the $HZnNH_2$ molecule lies 8.37 kcal mol^{-1} higher in energy than the $ZnNH_3$ complex (reaction 7). For the rearrangement of $ZnNH_3$ to $HZnNH_2$, the vibrational mode of the imaginary frequency of TS (1107.6i cm^{-1}) (Table 2) corresponds to the transition motion leading to the cleavage of the N–H bond. Transition-state optimization was followed by frequency and IRC calculations, which confirmed that TS does connect $ZnNH_3$ and $HZnNH_2$. Reactions 9 and 10 are predicted to be exothermic by about 63.20 and 36.33 kcal mol^{-1}, respectively, but require spin crossing.

For the cadmium system, there is no detectable $HCdNH_2$ produced in the present experiments, and $CdNH_3$ was the predominate product, implying that spin crossing has a higher efficiency in the $Zn + NH_3$ reaction system than that in the $Cd + NH_3$ reaction system. Spin crossing has also been observed in the isomerization of NH_3 by metal atoms (i.e. Zr, Hf, Ti, V, etc.).[2,22] On the other hand, the activation energy of the isomerization of $ZnNH_3$ ($^1A_1$) to $HZnNH_2$ ($^1A'$) (68.13 kcal mol^{-1}) is lower than that of the isomerization of $CdNH_3$ ($^1A_1$) to $HCdNH_2$ ($^1A'$) (80.02 kcal mol^{-1}) as shown in Fig. 5, indicating that the isomerization of NH_3 by Zn atoms is energetically more favorable than that by Cd. It is noted that the difference between the activation energy for the isomerization of MNH_3 ($^1A_1$) to $HMNH_2$ ($^1A'$) (M = Zn and Cd) corresponds to the energy difference between MNH_3 ($^1A_1$) and $HMNH_2$ ($^1A'$).

$$ZnNH_3\ (^1A_1) \rightarrow HZnNH_2\ (^1A')$$
$$\Delta E = 8.37\ \text{kcal mol}^{-1} \quad (7)$$

$$CdNH_3\ (^1A_1) \rightarrow HCdNH_2\ (^1A')$$
$$\Delta E = 34.61\ \text{kcal mol}^{-1} \quad (8)$$
$$ZnNH_3\ (^3A') \rightarrow HZnNH_2\ (^1A')$$
$$\Delta E = -63.20\ \text{kcal mol}^{-1} \quad (9)$$
$$CdNH_3\ (^3A') \rightarrow HCdNH_2\ (^1A')$$
$$\Delta E = -36.33\ \text{kcal mol}^{-1} \quad (10)$$

Conclusion

Reaction of zinc and cadmium atoms with ammonia molecules in solid-argon matrix has been studied by infrared spectroscopy and density functional theory calculations. From the infrared spectra, MNH_3 (M = Zn and Cd) mainly formed from the reaction of ammonia with the excited metal atoms, similar to the reaction of ammonia with excited Hg atom, but quite different from ground-state metal atoms such as Sc, Ti, V, etc. The absorptions of the inserted $HZnNH_2$ molecule sharply increased upon broad-band irradiation, whereas there was no detectable $HCdNH_2$ produced in the present experiments. The products were identified by isotopic substitution and density functional theoretical frequency calculations. As well, a number of novel species that have difficulty forming from the reactions with ground-state metals can be generated using excitation methods such as UV irradiation and laser ablation.

We would like to express our sincere thanks to the referee for valuable suggestions. We gratefully acknowledge financial support for this research by a Grant-in-Aid for Scientific Research (B) (Grant No. 17350012) from the Ministry of Education, Culture, Sports, Science and Technology (MEXT) of Japan and by Marubun Research Promotion Foundation. L.J. thanks MEXT of Japan and Kobe University for an Honors Scholarship.

References

1 See, for example: A. L. Casalnuova, J. C. Calabrese, D. Milstein, *Inorg. Chem.* **1987**, *26*, 971; R. Koelliker, D. Milstein, *J. Am. Chem. Soc.* **1991**, *113*, 8524; D. M. Roundmill, *Chem. Rev.* **1992**, *92*, 1; T. E. Muller, M. Beller, *Chem. Rev.* **1998**, *98*, 675; S. A. Macgregor, *Organometallics* **2001**, *20*, 1860.

2 M. H. Chen, H. Lu, J. Dong, L. Miao, M. F. Zhou, *J. Phys. Chem. A* **2002**, *106*, 11456.

3 J. W. Kauffman, R. H. Hauge, J. L. Margrave, *High Temp. Sci.* **1984**, *17*, 237.

4 J. Szczepanski, M. Szczesniak, M. Vala, *Chem. Phys. Lett.* **1989**, *162*, 123.

5 D. W. Ball, R. H. Hauge, J. L. Margrave, *High Temp. Sci.* **1988**, *25*, 95; D. W. Ball, R. H. Hauge, J. L. Margrave, *Inorg. Chem.* **1989**, *28*, 1599.

6 M. H. Chen, A. H. Zeng, H. Lu, M. F. Zhou, *J. Phys. Chem. A* **2002**, *106*, 3077.

7 M. C. Duval, B. Soep, R. D. van Zee, W. B. Bosma, T. S. Zwier, *J. Chem. Phys.* **1988**, *88*, 2148.

8 M. R. A. Blomberg, P. E. M. Siegbahn, M. Svensson, *Inorg. Chem.* **1993**, *32*, 4218.

9 See, for example: C. Xu, L. Manceron, J. P. Perchard, *J. Chem. Soc., Faraday Trans.* **1993**, *89*, 1291; V. E. Bondybey, A. M. Smith, J. Agreiter, *Chem. Rev.* **1996**, *96*, 2113; S. Fedrigo, T. L. Haslett, M. Moskovits, *J. Am. Chem. Soc.* **1996**, *118*, 5083; L. Khriachtchev, M. Pettersson, N. Runeberg, J. Lundell, M. Rasanen, *Nature* **2000**, *406*, 874; H. J. Himmel, L. Manceron, A. J. Downs, P. Pullumbi, *J. Am. Chem. Soc.* **2002**, *124*, 4448; J. Li, B. E. Bursten, B. Liang, L. Andrews, *Science* **2002**, *295*, 2242; L. Andrews, X. Wang, *Science* **2003**, *299*, 2049.

10 M. F. Zhou, N. Tsumori, Z. Li, K. Fan, L. Andrews, Q. Xu, *J. Am. Chem. Soc.* **2002**, *124*, 12936; M. F. Zhou, Q. Xu, Z. Wang, P. v. R. Schleyer, *J. Am. Chem. Soc.* **2002**, *124*, 14854; L. Jiang, Q. Xu, *J. Am. Chem. Soc.* **2005**, *127*, 42.

11 T. R. Burkholder, L. Andrews, *J. Chem. Phys.* **1991**, *95*, 8697; M. F. Zhou, N. Tsumori, L. Andrews, Q. Xu, *J. Phys. Chem. A* **2003**, *107*, 2458; L. Jiang, Q. Xu, **2005**, *122*, 034505.

12 M. J. Frisch, G. W. Trucks, H. B. Schlegel, G. E. Scuseria, M. A. Robb, J. R. Cheeseman, J. A. Montgomery, Jr., T. Vreven, K. N. Kudin, J. C. Burant, J. M. Millam, S. S. Iyengar, J. Tomasi, V. Barone, B. Mennucci, M. Cossi, G. Scalmani, N. Rega, G. A. Petersson, H. Nakatsuji, M. Hada, M. Ehara, K. Toyota, R. Fukuda, J. Hasegawa, M. Ishida, T. Nakajima, Y. Honda, O. Kitao, H. Nakai, M. Klene, X. Li, J. E. Knox, H. P. Hratchian, J. B. Cross, C. Adamo, J. Jaramillo, R. Gomperts, R. E. Stratmann, O. Yazyev, A. J. Austin, R. Cammi, C. Pomelli, J. W. Ochterski, P. Y. Ayala, K. Morokuma, G. A. Voth, P. Salvador, J. J. Dannenberg, V. G. Zakrzewski, S. Dapprich, A. D. Daniels, M. C. Strain, O. Farkas, D. K. Malick, A. D. Rabuck, K. Raghavachari, J. B. Foresman, J. V. Ortiz, Q. Cui, A. G. Baboul, S. Clifford, J. Cioslowski, B. B. Stefanov, G. Liu, A. Liashenko, P. Piskorz, I. Komaromi, R. L. Martin, D. J. Fox, T. Keith, M. A. Al-Laham, C. Y. Peng, A. Nanayakkara, M. Challacombe, P. M. W. Gill, B. Johnson, W. Chen, M. W. Wong, C. Gonzalez, J. A. Pople, *Gaussian 03, Revision B.04*, Gaussian, Inc., Pittsburgh, PA, **2003**.

13 C. Lee, E. Yang, R. G. Parr, *Phys. Rev. B* **1988**, *37*, 785; A. D. Becke, *J. Chem. Phys.* **1993**, *98*, 5648.

14 A. D. McLean, G. S. Chandler, *J. Chem. Phys.* **1980**, *72*, 5639; R. Krishnan, J. S. Binkley, R. Seeger, J. A. Pople, *J. Chem. Phys.* **1980**, *72*, 650; M. J. Frisch, J. A. Pople, J. S. Binkley, *J. Chem. Phys.* **1984**, *80*, 3265; A. J. H. Wachters, *J. Chem. Phys.* **1970**, *52*, 1033; P. J. Hay, *J. Chem. Phys.* **1977**, *66*, 4377.

15 P. J. Hay, W. R. Wadt, *J. Chem. Phys.* **1985**, *82*, 299.

16 S. Suzer, L. Andrews, *J. Chem. Phys.* **1987**, *87*, 5131.

17 V. A. Macrae, T. M. Greene, A. J. Downs, *Phys. Chem. Chem. Phys.* **2004**, *6*, 4586.

18 T. M. Greene, W. Brown, L. Andrews, A. J. Downs, G. V. Chertihin, N. Runeberg, P. Pyykkö, *J. Phys. Chem.* **1995**, *99*, 7925.

19 W. H. Breckenridge, J. H. Wang, *J. Chem. Phys.* **1987**, *87*, 2630.

20 T. M. Greene, L. Andrews, A. J. Downs, *J. Am. Chem. Soc.* **1995**, *117*, 8180.

21 L. Jiang, Q. Xu, *J. Am. Chem. Soc.* **2005**, *127*, 8906.

22 M. F. Zhou, M. H. Chen, L. N. Zhang, H. Lu, *J. Phys. Chem. A* **2002**, *106*, 9017.